Published in final edited form as:
Langmuir. 2008 June 1; 24(13): 6721–6729. doi:10.1021/la8005772.

Determination of the Adsorption Free Energy for Peptide–Surface Interactions by SPR Spectroscopy

Yang Wei and **Robert A. Latour***
Department of Bioengineering, 501 Rhodes Engineering Research Center, Clemson University, Clemson, South Carolina 29634

Abstract

To understand and predict protein adsorption behavior, we must first understand the fundamental interactions between the functional groups presented by the amino acid residues making up a protein and the functional groups presented by the surface. Limited quantitative information is available, however, on these types of submolecular interactions. The objective of this study was therefore to develop a reliable method to determine the standard state adsorption free energy ($\Delta G°_{ads}$) of amino acid residue–surface interactions using surface plasma resonance (SPR) spectroscopy. Two problems are commonly encountered when using SPR for peptide adsorption studies: the need to account for "bulk-shift" effects and the influence of peptide–peptide interactions at the surface. Bulk-shift effects represent the contribution of the bulk solute concentration to the SPR response that occurs in addition to the response due to adsorption. Peptide–peptide interactions, which are assumed to be zero for Langmuir adsorption, can greatly skew the isotherm shape and result in erroneous calculated values of $\Delta G°_{ads}$. To address these issues, we have developed a new approach for the determination of $\Delta G°_{ads}$ using SPR that is based on the chemical potential. In this article, we present the development of this new approach and its application for the calculation of $\Delta G°_{ads}$ for a set of peptide–surface systems where the peptide has a host–guest amino acid sequence of TGTG-X-GTGT (where G and T are glycine and threonine residues and X represents a variable residue) and the surface consists of alkanethiol self-assembled monolayers (SAMs) with methyl (CH_3) and hydroxyl (OH) functionality. This new approach enables bulk-shift effects to be directly determined from the raw SPR versus peptide concentration data plots and the influence of peptide–peptide interaction effects to be minimized, thus providing a very straightforward and accurate method for the determination of $\Delta G°_{ads}$ for peptide adsorption. Further studies are underway to characterize $\Delta G°_{ads}$ for a large library of peptide–SAM combinations.

I. Introduction

It is widely recognized that protein–surface interactions are of fundamental importance in the field of biomaterials because of the governing role that they play in the biological response to an implanted material.[1-5] To understand the importance of these events, it is first necessary to recognize that cells in the body generally do not have receptors for synthetic materials and thus lack the inherent ability to respond directly to chemically stable materials that are made from nonbiologically based plastics, metals, or ceramics. However, when these types of materials are implanted in the body, proteins that are soluble in the blood and interstitial fluids rapidly coat the surface of the implant. This represents the critical event that makes the implant surface bioactive. Cellular response to an implanted material is then dictated by the types of proteins that adsorb to the implant's surface and the bioactive state of those proteins, which, in turn, is directly influenced by the protein adsorption process.[6,7] Unfortunately, it has proven to be

* To whom correspondence maybe addressed. E-mail: latourr@clemson.edu.

extremely difficult to understand and control these types of interactions quantitatively because of the complexities involved.[8-10] On a fundamental level, however, protein adsorption behavior can be considered to be represented by the combination of the individual interactions among the amino acid residues making up a protein (of which there are 20 different types coded for by DNA), the solvent environment (i.e., water molecules, salt ions, and pH), and the functional groups presented by a surface. These types of interactions can be characterized by the change in standard-state free energy associated with their adsorption to a functionalized surface ($\Delta G°_{ads}$), with this information then used to provide an initial understanding of the submolecular events that govern protein adsorption behavior.

Vernekar and Latour developed one of the first experimental model systems for the determination of $\Delta G°_{ads}$ for peptide–surface interactions using surface plasmon resonance (SPR) spectroscopy.[6] They used a G_4-X-G_4 host–guest model peptide system on OH- and COOH-functionalized gold–alkanethiol self-assembled monolayer (SAM) surfaces, where G represents glycine and X was either glycine (G) or lysine (K) using the standard one-letter amino acid code. With this system, the G_4-K-G_4 peptide was found to exhibit a very strong adsorption response on the COOH–SAM surface, with a $\Delta G°_{ads}$ value of −6.9 ± 0.2 kcal/mol (mean ± 95% confidence interval (CI)) at 25 °C obtained by fitting a Langmuir adsorption model to the adsorption isotherms. The other three systems (G_4-K-G_4 on the OH–SAM and G_4-G-G_4 on both the OH– and COOH–SAMs) exhibited no detectable adsorption response. This prevented the fitting of the Langmuir model to the data, with $\Delta G°_{ads}$ then simply considered to be zero for each of these systems because of the lack of a measureable response. Along with the initial development and application of a method using SPR to determine $\Delta G°_{ads}$ for peptide–SAM systems, their study also identified several limitations with the approach that was initially developed. First, the G_4-X-G_4 form of the host–guest peptide was determined to possess very limited solution solubility when G was used for the guest residue (i.e., X = G), and its overall peptide molecular weight was fairly small, which limited the sensitivity of the detection of adsorption events using SPR. Second, the method used by Vernekar and Latour required the use of the OH–SAM surface, which was determined to be nonadsorbing, to measure the bulk-shift effects that were then used for the correction of the COOH–SAM surface data. Although this was a reasonable assumption for the systems evaluated, it added complexity and a potential source of error to the method. Third, because the Langmuir model used in their study could not be fit to an isotherm that exhibited nearly zero adsorption, the free energy of adsorption for weakly adsorbing systems could not be directly determined by their method but instead had to be assumed to have a zero value. Although not addressed by Vernekar and Latour, their method also provided no means to address differences in peptide–peptide interactions at the surface but simply assumed that these types of interactions did not occur. Similar methods to these have also been used by Husson et al.[11,12] for the measurement of a broader selection of peptide–surface combinations, with their studies having the same limitations as the prior study by Vernekar and Latour.

To address these problems, we have further developed the experimental system initially designed by Vernekar and Latour by using a chemical potential approach to solve each of the previously encountered problems. We have redesigned the host–guest peptide model for improved solubility and detection by SPR, developed a direct method to account for bulk-shift effects for each individual peptide–surface system, revised the adsorption model for use with SPR isotherm data to enable adsorption free energy to be directly determined for even very weakly interacting systems, and developed a method to minimize the effects of peptide–peptide interactions for the calculation of $\Delta G°_{ads}$. In this article, we present this revised approach, demonstrate its use to determine the adsorption free energy for a new set of peptide–SAM surface systems, and address various experimental factors and their influence when conducting these types of experiments with SPR.

II. Analytical Model

II.a. Key Issues

To determine ΔG°_{ads} accurately for peptide adsorption using SPR, two key issues must be addressed: the need to account for (1) "bulk-shift" effects and (2) the influence of solute–solute interactions on the surface.

Because SPR measures the refractive index change of the medium within a distance of about 300 nm of the surface,[13] it is sensitive to both the molecules adsorbed at the interface and the molecules suspended in the medium.[13] This latter contribution, known as the "bulk effect", introduces a component into the SPR signal that is linearly proportional to the mass concentration of the analyte in the solution.[14] Therefore, to determine the amount of SPR signal that is due to the adsorption process, the bulk shift contribution must be subtracted from the raw SPR signal that is obtained during the adsorption experiment.

Peptide–peptide interactions present another problem that can greatly skew the shape of the adsorption isotherm and result in erroneous calculated values of ΔG°_{ads}. ΔG°_{ads} is determined from the equilibrium constant, K_{eq}, of a reversible adsorption process, which represents the partition coefficient for the concentration of the solute on a surface versus its concentration in bulk solution. Ideally, the value of K_{eq} could be determined as the initial slope in the linear region of the adsorption isotherm, which represents infinite dilution conditions, in order to minimize effects from solute–solute interactions at the surface.[15] Unfortunately, this requires the measurement of adsorption events for solution concentrations that typically extend well below the detection limit of currently available commercial SPR instruments. To get around this problem, an adsorption model, such as the Langmuir model, is generally used to calculate ΔG°_{ads} on the basis of the overall shape of the isotherm. This, however, creates additional complications because solute–solute interactions may occur on the surface as the surface sites become filled, which can substantially influence the shape of the isotherm and invalidate the application of the Langmuir adsorption model. If the Langmuir model is still used despite the occurrence of solute–solute interactions, then substantial error will be introduced into the calculated value of ΔG°_{ads}.[16-22]

To address both of these problems, we have adapted our analytical model to enable bulk-shift contributions to be directly determined from the raw SPR signal versus solution concentration plots for each individual peptide–surface system and to enable the effects of solute–solute interactions on the isotherm shape to be minimized so that ΔG°_{ads} can be accurately determined from the resulting adsorption data.

II.b. Model Development

For a reversible adsorption process under equilibrium conditions, the chemical potential of an adsorbed peptide must be equal to its chemical potential in solution, which can be expressed as[23]

$$\mu_s=\mu_b \quad \text{with} \quad \mu=\mu^o+RT\ln(a) \quad \text{and} \quad a=\gamma C/C^o$$
$$\mu_s=\mu_s^o+RT\ln(\gamma_s C_s/C^o)=\mu_b=\mu_b^o+RT\ln(\gamma_b C_b/C^o)$$

Under dilute conditions, $\gamma \approx 1.0$, and defining $C^\circ = 1.0$ M gives

$$\Delta\mu^o=\mu_s^o-\mu_b^o=-RT\ln(C_s/C_b)=\Delta G_{ads}^o \tag{1}$$

where μ is the chemical potential of the peptide, superscript "o" designates standard-state conditions, subscripts s and b designate the states of the peptide when it is adsorbed to the surface or in bulk solution, respectively, a and γ are the activity and the activity coefficient of the peptide, respectively, C is the concentration of the peptide, and R and T are the ideal gas constant and absolute temperature, respectively.

The concentration of the peptide at the surface (C_s) can be expressed as

$$C_s = q/\delta + C_b \tag{2}$$

where q is the excess amount of peptide per unit area adsorbed on the surface compared to that under bulk solution conditions (i.e., C_b) and δ is the thickness of the adsorbed layer.

The excess amount of solute adsorbed to the surface, q, can be directly measured by SPR and related to the standard parameters that are used to characterize an adsorption process, which can be expressed as[1]

$$P + S \rightleftharpoons PS \tag{3}$$

where, P, S, and PS represent the peptide in solution, the available surface sites for peptide adsorption, and the adsorbed peptide on the surface, respectively. Assuming a reversible adsorption process and again assuming unity activity coefficients, the change in the free energy of the adsorption process can be expressed as[1,6,11,24]

$$K = \left(\frac{x_{PS}}{a_P x_S}\right) = \frac{q/Q}{\left(\frac{C_b}{C^o}\right)\frac{(Q-q)}{Q}}$$

$$\text{which can be rearranged to} \quad q = \frac{QC_b}{C_b + C^o K^{-1}} \tag{4}$$

where K is the equilibrium constant for the adsorption reaction expressed in eq 3, x_{PS} and x_S are the mole fractions of surface sites occupied and unoccupied by the peptide, respectively, and Q is amount of peptide adsorbed at surface saturation. The final expression represented by eq 4 represents the classic Langmuir adsorption model.[25-29]

During an SPR experiment to measure the adsorption of a peptide to a surface, the overall change in the SPR signal reflects both the excess amount of adsorbed peptide, q, and the bulk shift response, which is linearly proportional to the concentration of peptide in solution.[14] This can be expressed as

$$\text{SPR} = q + mC_b = \frac{QC_b}{C_b + C^o K^{-1}} + mC_b \tag{5}$$

where m is the proportionality constant between the peptide concentration in the bulk solution and the bulk shift in the SPR response. Equation 5 can be directly fit to a plot of the raw SPR signal versus peptide solution concentration, C_b, to solve for the parameters of Q, K, and m, which enables bulk-shift effects (represented by mC_b) to be directly accounted for by each individual peptide–surface system.

As introduced above, however, fitting the Langmuir adsorption model to a solute adsorption isotherm has the inherent problem that the shape of the isotherm is often influenced by solute–solute interactions, with the subsequent values of Q and K in eqs 4 and 5 being directly affected,

in which case the value of K may not provide an accurate representation of ΔG°_{ads}. Solute–solute effects are minimized, however, when adsorption takes place under the condition where the bulk solution concentration (C_b) approaches zero. As shown from the last expression in eq 4, under this condition the relationship between q and C_b becomes

$$(q)_{C_b \to 0} = \left(\frac{QK}{C^{o}}\right) C_b \tag{6}$$

with q thus being linearly related to C_b under these conditions. Unfortunately, the relationship between q and C_b at very low concentrations is not experimentally accessible because of the sensitivity limitations of SPR. However, the adsorption behavior can still be determined under these conditions using the values of Q and K obtained from fitting eq 5 to the SPR response over the experimentally accessible range of peptide solution concentrations, with these values then plugged into eq 6 to calculate $(q)_{C_b \to 0}$. By this approach, Q and K essentially serve only as fitting parameters for the purpose of estimating the linear response of the isotherm plot as C_b approaches zero. Therefore, while the influence of solute–solute interactions may affect the actual values of Q and K, they should not influence the ability of Q and K to serve as fitting parameters to estimate the initial slope of the isotherm, thus separating the effects of solute–solute interactions from the determination of ΔG°_{ads}, as addressed in the following paragraph.

Equation 6 can now be combined with eqs 1 and 2 to derive an expression for the chemical potential based on the experimentally determined parameters Q and K for situation in which C_b approaches zero, thus minimizing peptide–peptide interactions, which gives

$$\begin{aligned} &(C_s)_{C_b \to 0} = (q)_{C_b \to 0}/\delta + C_b = \left(\frac{QK}{\delta C^{o}}\right) C_b + C_b = \left(\frac{QK}{\delta C^{o}} + 1\right) C_b \\ &\text{with} \quad \Delta G^{o}_{ads} = -RT \ln\left[(C_s)_{C_b \to 0}/C_b\right] = -RT \ln\left(\frac{QK}{\delta C^{o}} + 1\right) \end{aligned} \tag{7}$$

Equation 7 thus provides a relationship for the determination of ΔG°_{ads} for peptide adsorption to a surface with a minimal influence of peptide–peptide interactions based on experimentally determined parameters Q and K and the theoretically defined parameter δ.

We will next address how δ is determined and evaluate the sensitivity of the calculated values of ΔG°_{ads} to the value of this parameter.

The δ parameter is determined by assuming that its value is equal to twice the average outer radius of the peptide, with the peptide represented as being spherical in shape. Under these assumptions, a peptide's volume can be estimated from its molecular weight and the average value of a protein's molar specific volume in solution. The average experimentally determined molar specific volume for a soluble peptide or protein is approximately 0.73 cm^3/g.[30] For a TGTG-X-GTGT peptide with X representing an amino acid with an average residue molecular weight of M_w = 118.9 Da,[31] which results in M_w = 769.3 Da for the peptide, the value of R_{pep} (radius of a peptide molecule) is calculated as[32]

$$\begin{aligned} &V_{pep} = \frac{4}{3}\pi R_{pep}{}^3 = \left(0.73 \frac{cm^3}{g}\right)\left(\frac{M_w}{N_{Av}}\right) \text{or} \\ &R_{pep} = \left[\frac{3}{4\pi}\left(0.73 \frac{cm^3}{g}\right)\left(\frac{M_w}{N_{Av}}\right)\left(\frac{10^{24} \text{ Å}}{cm^3}\right)\right]^{1/3} = 6.06 \quad \text{Å} \end{aligned} \tag{8}$$

which gives $\delta = 2R_{pep}$ = 12.1 Å, where V_{pep} is the molecular volume of the peptide and N_{Av} is Avogadro's number. Molecular dynamics simulations with similar peptides[33] show this to be a very reasonable value for the adsorbed layer of this peptide.

Although it would be ideal not to have to rely on the use of a theoretically derived parameter for the calculation of $\Delta G°_{ads}$, it can be shown that the value of $\Delta G°_{ads}$ is actually fairly insensitive to the value of δ. The sensitivity of $\Delta G°_{ads}$ to the value of δ can be evaluated by assessing how $\Delta G°_{ads}$ is affected by the value of δ under different conditions of adsorption. Equation 7 provides the relationship between $\Delta G°_{ads}$ and δ, and the differentiation of eq 7 with respect to δ gives

$$\frac{\mathrm{d}}{\mathrm{d}\delta}\left(\Delta G^{\mathrm{o}}_{\mathrm{ads}}\right)=RT\left(\frac{QK}{(QK+\delta C^{\mathrm{o}})\,\delta}\right) \tag{9}$$

For the case of a relatively strongly adsorbing system (e.g., when $QK \gg \delta C°$), eqs 7 and 9 respectively become

$$\left[\Delta G^{\mathrm{o}}_{\mathrm{ads}}\right]_{QK\gg\delta C^{\mathrm{o}}}=\left[-RT\ln\left(\frac{QK}{\delta C^{\mathrm{o}}}+1\right)\right]_{QK\gg\delta C^{\mathrm{o}}}\approx -RT\ln\left(\frac{QK}{\delta C^{\mathrm{o}}}\right) \tag{10}$$

$$\text{and}\left[\frac{\mathrm{d}}{\mathrm{d}\delta}\left(\Delta G^{\mathrm{o}}_{\mathrm{ads}}\right)\right]_{QK\gg\delta C^{\mathrm{o}}}=RT\left[\frac{QK}{(QK+\delta C^{\mathrm{o}})\,\delta}\right]_{QK\gg\delta C^{\mathrm{o}}}\approx\frac{RT}{\delta} \tag{11}$$

As an example of what these expressions represent, for the situation where T = 298 K and $QK = 5\delta C°$, the value of $\Delta G°_{ads}$ is equal to about −1.0 kcal/mol, with $\Delta G°_{ads}$ becoming even more negative for a larger of $QK/\delta C°$ ratio. Using the value of δ calculated from eq 8 (i.e., δ = 12.1 Å), eq 11 shows that the sensitivity of $\Delta G°_{ads}$ to the value of δ is only $\mathrm{d}(\Delta G°_{ads})/\mathrm{d}\delta$ = 0.050 kcal/mol/Å. It should also be noted that under these conditions the difference between $\Delta G°_{ads}$ for two different peptide–surface systems (i.e., $\Delta\Delta G°_{ads}$) becomes

$$\Delta\Delta G^{\mathrm{o}}_{\mathrm{ads}}=\left(\Delta G^{\mathrm{o}}_{\mathrm{ads}}\right)_2-\left(\Delta G^{\mathrm{o}}_{\mathrm{ads}}\right)_1=-RT\ln\left(\frac{(QK)_2}{(QK)_1}\right) \tag{12}$$

in which case the parameter δ divides out of the relationship altogether. Taking the other extreme condition (i.e., when $QK \ll \delta C°$), eqs 7 and 9, respectively, become

$$\left[\Delta G^{\mathrm{o}}_{\mathrm{ads}}\right]_{QK\ll\delta C^{\mathrm{o}}}=\left[-RT\ln\left(\frac{QK}{\delta C^{\mathrm{o}}}+1\right)\right]_{QK\ll\delta C^{\mathrm{o}}}\approx -RT\ln(1)=0 \tag{13}$$

$$\text{and}\left[\frac{\mathrm{d}}{\mathrm{d}\delta}\left(\Delta G^{\mathrm{o}}_{\mathrm{ads}}\right)\right]_{QK\ll\delta C^{\mathrm{o}}}=RT\left[\frac{QK}{(QK+\delta C^{\mathrm{o}})\,\delta}\right]_{QK\ll\delta C^{\mathrm{o}}}\approx\frac{RT}{\delta}\left(\frac{QK}{\delta C^{\mathrm{o}}}\right)\approx 0 \tag{14}$$

As an example of what these relationships show, under the conditions of T = 298 K and $QK = (1/5)\delta C°$, is $\Delta G°_{ads} \approx -0.1$ kcal/mol and $\mathrm{d}(\Delta G°_{ads})/\mathrm{d}\delta$ = 0.008 kcal/mol/Å. Finally, to consider the influence of the values of δ for the case where the value of $\Delta G°_{ads}$ is between −1.0 and 0.0 kcal/mol (e.g., when $QK \approx \delta C°$), the sensitivity of the value of $\Delta G°_{ads}$ to the change in δ can be expressed as

$$\left[\Delta G^{\circ}_{\text{ads}}\right]_{QK=\delta C^{\circ}} = \left[-RT\ln\left(\frac{QK}{\delta C^{\circ}}+1\right)\right]_{QK=\delta C^{\circ}} \approx -RT\ln(2) = -0.41 \quad \text{kcal/mol} \tag{15}$$

$$\left[\frac{\mathrm{d}}{\mathrm{d}\delta}\left(\Delta G^{\circ}_{\text{ads}}\right)\right]_{QK\approx\delta C^{\circ}} = RT\left[\frac{QK}{(QK+\delta C^{\circ})\,\delta}\right]_{QK\approx\delta C^{\circ}} \approx \frac{RT}{2\delta} \tag{16}$$

When $QK = \delta C^{\circ}$ (in which case $\Delta G^{\circ}_{\text{ads}} = -0.4$ kcal/mol) and when using the calculated value of $\delta = 12.1$ Å, the expression in eq 16 shows a sensitivity of only $\mathrm{d}(\Delta G^{\circ}_{\text{ads}})/\mathrm{d}\delta = 0.025$ kcal/mol/Å. These analyses thus show that $\Delta G^{\circ}_{\text{ads}}$ is fairly insensitive to the value calculated for the theoretical parameter δ, and when comparing $\Delta G^{\circ}_{\text{ads}}$ values between two at least moderately strongly adsorbing systems (i.e., for cases where $\Delta G^{\circ}_{\text{ads}} < -1.0$ kcal/mol), the value of $\Delta\Delta G^{\circ}_{\text{ads}}$ is not dependent on the value of δ at all.

III. Experimental Methods

III.a. Methods Overview

As introduced above, our adsorption studies were conducted using a host–guest model peptide on functionalized gold–alkanethiol SAM surfaces. Adsorption isotherms for each peptide–SAM surface system were generated by recording the adsorption response by SPR over a range of solution concentrations, and a value for $\Delta G^{\circ}_{\text{ads}}$ was then calculated for each system using the adsorption model described in section II.

III.b. Host–Guest Peptide Model

For our adsorption studies, we designed and had synthesized (SynBioSci Corporation, Livermore, CA) a unique model peptide system in the form of TGTG-X-GTGT with zwitterionic end groups, where G and T are glycine (-H side chain) and threonine (-$CH(CH_3)$OH side chain) and X represents the "guest" amino acid residue, which can be selected among any of the 20 naturally occurring amino acid types. The threonine residues and the zwitterionic end groups were selected to enhance aqueous solubility and provide additional molecular weight for SPR detection whereas the nonchiral glycine residues were selected to inhibit the formation of secondary structure, which, if present, would complicate the adsorption process and make the data more difficult to understand. The variable X residue was positioned in the middle of the peptide to best represent the characteristics of a midchain amino acid in a protein by positioning it relatively far from the zwitterionic end groups. In this initial set of adsorption studies, three different types of amino acids were used for the X residue to vary the overall characteristics of the peptides, with X represented by either threonine (T; -$CH(CH_3)$OH side chain, polar character), aspartic acid (D; -CH_2COOH side chain, negatively charged, pK = 3.9 [34]), or valine (V; -$CH(CH_3)_2$ side chain, nonpolar character). Each of these three peptides was synthesized and characterized by analytical HPLC and mass spectral analysis by SynBioSci Corporation (Livermore, CA), which showed that all of the peptides were ≥98% pure.

III.c. SAM Surfaces

The structural characteristics of SAMs are well known, and standard procedures were followed while preparing our SAM surfaces,[35,36] which we will summarize. The OH- and CH_3-terminated Au–alkanethiol SAMs were synthesized from 11-mercapto-1-undecanol and 1-dodecanethiol (Aldrich Chemical Co., Milwaukee, WI), respectively. The alkanethiols were dissolved separately in ethanol (anhydrous (100%), denatured ethyl alcohol, Fisher Scientific, Fair Lawn, NJ) to obtain 1 mM ethanolic solutions in preparation for SAM fabrication on gold

surfaces. The bare gold surfaces for the SPR experiments were purchased from Biacore (SIA Au kit, BR-1004−05, Biacore, Inc., Uppsala, Sweden). Prior to use, the surfaces were thoroughly cleaned by immersion into 50 °C piranha solution (70% concentrated H_2SO_4 (Fisher Scientific, Fair Lawn, NJ) and 30% hydrogen peroxide (Fisher Scientific, Fair Lawn, NJ)) for 1 min and were rinsed with nanopure water. The surfaces were then immersed in a 50 °C ammonia solution (20% NH_4OH (Fisher Scientific, Fair Lawn, NJ) and 20% hydrogen peroxide with 60% DI water) for 1 min, rinsed with nanopure DI water, dried under a steady stream of nitrogen gas (National Welders Supply Co., Charlotte, NC), and then immersed in clean glass vials with each containing a 1.0 mM solution of either OH- or CH_3-terminated alkanethiols in ethanol. Each container was then backfilled with dry nitrogen gas and sealed. The SAM-coated gold surfaces were stored in the solutions in a dark environment (at least 24 h) until used to prepare the biosensor surfaces. Before an adsorption experiment, each SAM biosensor surface was ultrasonically cleaned (Branson Ultrasonic Corporation, Danbury, CT) for 5 s in ethanol, rinsed copiously with ethanol and then nanopure DI water, and then dried thoroughly in a stream of nitrogen gas. The SAM sensor chip was then mounted on the cartridge that goes into the SPR instrument, docked with the SPR microfluidics channel, and promptly used in an adsorption experiment. Prior to our adsorption studies, each type of SAM surface was also characterized by ellipsometry (GES 5 variable-angle spectroscopic ellipsometer, Sopra Inc., Palo Alto, CA), contact angle (CAM 200 optical contact-angle goniometer, KSV Instruments Inc., Monroe, CT), and X-ray photoelectron spectroscopy (XPS, performed at NESCA/BIO, University of Washington, Seattle, WA). All XPS spectra were taken on a Surface Science Instruments S-probe spectrometer. The Service Physics ESCAVB Graphics Viewer program was used to calculate the elemental compositions from peak area.

III.d. SPR Adsorption Experiments

Adsorption experiments were conducted by SPR using a Biacore × instrument (Biacore, Inc., Piscataway, NJ). To maintain the experimental solutions of the peptides at a pH of 7.4, 10 mM phosphate-buffered saline (PBS) (140 mM NaCl, pH 7.4) (Fisher Scientific, Fair Lawn, NJ) was used as the running buffer. Before every SPR experiment, the buffer solution was filtered with a vacuum filter system (Corning Costar, Corning, NY), followed by gentle heating for 15 min at 40 °C under a vacuum of 270−280 mmHg (Laboratory-Line Duo-Vac Oven, Laboratory-Line Instruments, Inc., Melrose Park, IL) and sonication for 5 min for degassing.

Eight concentrations of each of the peptide solutions (0.039, 0.078, 0.156, 0.312, 0.625, 1.25, 2.5, and 5.0 mg/mL) were prepared in the filtered and degassed 10 mM phosphate-buffered saline through serial dilutions from stock solutions of the peptide in clean vials. The pH of the stock solutions was adjusted to 7.4 with 0.1 M NaOH (Sigma Chemical Co., St. Louis, MO) or 0.1 M HCl (Mallinckrodt Chemical, Inc., Paris, KY). The actual concentration of the stock peptide solution was calibrated by BCA analysis (BCA protein assay kit, prod. 23225, Pierce, Rockford, IL) against a BSA standard curve, and the diluted concentration of each peptide was further validated from a refractive index versus diluted concentration plot using a refractive index meter (AR 70 automatic refractometer, Reichert, Inc., Depew, NY).

Once the biosensor SAM chip was docked inside the SPR instrument, the microfluidics flow channels exposed to the SAM surface were flushed with the PBS solution at a flow rate of 50 μL/min for 2 to 3 min, followed by two surface preparation/regeneration injections that involved a 50 μL injection of 0.3 vol % Triton X-100 (Sigma Chemical Co., St. Louis, MO), followed by a “wash” operation (flushing buffer at high flow rate through the microfluidics system for approximately 2 min). This is a standard procedure that has been demonstrated to provide very stable and repeatable responses for peptide adsorption measurements using this instrument.

After the initial surface preparation step was conducted and a stable SPR sensorgram trace was obtained, each surface was finally prepared for an adsorption measurement by running 50 μL of concentrated peptide solution injections (5.0 mg/mL) over the SAM surface several times, followed by a PBS wash until a fully reversible adsorption signal was obtained. Preliminary studies have shown that by this process a small amount of peptide (typically less than a few percent of a monolayer) is irreversibly bound to each SAM surface, with this peptide believed to be adsorbed at defects sites (e.g., grain boundaries, step defects, and vacancy defects) in the SAM surface. Pretreatment of the surface in this manner enables these defect sites to be blocked by irreversibly bound peptide, with the remaining SAM surface exhibiting reversible adsorption behavior. Following this final surface pretreatment step, eight different concentrations of each peptide solution were injected over each functionalized-SAM SPR chip in random order at a flow rate of 50 μL/min, followed by 50 μL/min PBS buffer flow to desorb the peptide from the surface. Then a blank buffer injection was administered to flush the injection port, and a set of regeneration injections were then performed to prepare the surface for the next series of peptide sample injections. Our previous studies have shown that these conditions provide for an adsorption process that is not mass-limited and results in no detectable level of degradation of the SAM surface.[6]

SPR sensorgrams in the form of resonance units (RU; 1 RU = 1.0 pg/mm^2)[13] vs time were recorded for six independent runs of each series of peptide concentrations over each SAM surface at 25 °C and the data were then used to generate isotherm curves for analysis by plotting the raw SPR signal vs peptide solution concentration. Equation 5 was then best-fitted to each isotherm plot by nonlinear regression to solve for the parameters of Q, K, and m using the Statistical Analysis Software program (SAS Institute, Cary, NC). The values of Q and K were then used in eq (7) for the calculation of $\Delta G°_{ads}$ for each peptide–SAM system, with the value of δ calculated for each peptide using eq (8) (value of δ given in Table 1).

IV. Results and Discussion

IV.a. Surface Characterization

Table 2 presents surface characterization data for the SAM surfaces, which show that the contact angle and thickness values fall within the expected range for these types of surfaces.[10,37-43] These results confirm that the OH– and CH_3–SAMs represent very hydrophilic and hydrophobic surfaces, respectively, which should thus exhibit distinctly different adsorption characteristics for the host–guest peptides.

Table 3 presents the atomic composition for the OH- and CH_3-terminated SAMs from XPS. Composition scans for the CH_3 and OH surfaces showed minimal levels of contamination with a gold signal that is consistent with a 11- to 12-carbon alkanethiol SAM layer on gold and with the compositions found to be in excellent agreement with theoretical values for these surface types.

IV.b. SPR Adsorption Analysis

Figure 1 shows the raw SPR adsorption curves on a mass basis for each peptide on the OH– and CH_3–SAM surfaces. As shown, a rapidly rising signal response is generated as soon as the peptide solution begins to flow over the surface. This rise is due to a combination of the bulk-shift effect, which is linearly proportional to the concentration of the peptide in solution over the surface,[14] and the excess concentration of the peptide on the surface due to adsorption. The SPR signal then stabilizes, which indicates that an equilibrated state has been achieved in which the rate of peptide adsorption onto the surface is equal to the rate of desorption off of the surface. It should be noted here that a slight amount of instrument drift also occurs during this time, with the amount of drift being consistent for each peptide–SAM combination and at

each concentration. This effect gives the appearance of a small continual increase in the SPR signal even after equilibrium is achieved; this issue is further addressed in section IV.c. Following equilibration, the surface was exposed to the pure buffer solution at the same flow rate as was used for the peptide sample, which results in a rapid drop in signal due to the bulk shift effect. This response is followed by an exponentially decaying signal, which represents the desorption of the peptide from the surface.

The reversibility of each adsorption process was assessed by comparing the SPR signal before the injection of peptide solution and after the period of desorption. Reversibility represents an essential condition for the application of eqs 1-7 to the adsorption data for the calculation of adsorption free energy from the adsorption isotherms. The data presented in Figure 1 clearly show that the adsorption process for each of our peptide–SAM systems was fully reversible. The differences in the SPR signals before the injection of peptide solution and after desorption typically are less than 20 RUs, with these small measured differences being attributed to instrument drift. The combination of an adsorption process that reaches an equilibration plateau followed by a desorption process that is completely reversible satisfies the necessary conditions for the determination of $\Delta G°_{ads}$ for each of our peptide–SAM systems.

Adsorption isotherms for each of the peptide–SAM systems, which are shown in Figure 2, were generated from the raw experimental data shown in Figure 1 by plotting the changes in RU versus peptide solution concentration. Figure 2 also shows the best-fit curves for eq 5. Values of the parameters *Q*, *K*, and *m* were determined by nonlinear regression using SAS and these values were then used to calculate $\Delta G°_{ads}$ for each peptide–SAM system using eq 7. The resulting values for *Q*, *K*, *m*, and $\Delta G°_{ads}$ are presented in Table 4, with *Q* and *K* serving to characterize the shape of the isotherm, *m* representing the bulk–shift effect, and $\Delta G°_{ads}$ being the calculated standard-state adsorption free energy.

The results presented in Table 4 for $\Delta G°_{ads}$ and show that the hydrophilic OH–SAM was essentially nonadsorptive to these peptides with the absolute magnitude of $\Delta G°_{ads}$ being less than 0.005 kcal/mol for each system. This behavior can be understood to result from the stronger tendency of the hydroxyl functional groups on the SAM surface and the hydrogen-bondable groups of the peptides to form hydrogen bonds with the surrounding water molecules compared to their tendency to form hydrogen bonds with one another. In contrast, the hydrophobic CH_3–SAM strongly adsorbed the peptides with the values of $\Delta G°_{ads}$ for each peptide on this surface being significantly lower than on the OH–SAM surface ($p < 0.01$). In addition, the adsorption behavior of each peptide on the CH_3–SAM surface was also significantly different ($p < 0.01$), which shows that the use of this peptide model enables the effects of the midchain amino acid residues to be clearly discerned. These results are in excellent agreement with past theoretical studies that have been conducted by our group using semiempirical quantum chemical calculations[44-46] and molecular dynamics simulations[33, 47] to evaluate the interactions between different amino acid residues and functional groups presented by SAM surfaces.

For comparison sake, we also calculated values of the standard-state free energy, $\Delta G°_{Langmiur}$, using the conventional Langmuir isotherm method from the following relationship:

$$\Delta G^{o}_{Langmuir} = -RT\ln(K) \tag{17}$$

where the values of *K*, which are presented in Table 4, were determined from fitting eq 4 to Langmuir isotherm data (i.e., *q* vs C_b). The most striking difference between the values of adsorption free energy between these two methods is seen for the OH–SAM surface, where $\Delta G°_{Langmiur}$ is calculated to be about −1.75 kcal/mol and $\Delta G°_{ads}$ calculated by the new method

is very close to 0.00 kcal/mol. As shown in Figure 2, the amount of peptide adsorbed on the OH–SAM surface is barely detectable above the bulk shift response, which indicates a very weak interaction for this surface. This then also represents a system where peptide–peptide interactions can be expected to substantially inhibit the adsorption of peptides to neighboring sites on the surface. In fact, as shown in Table 4, the value of the *Q* parameter for this surface, which represents the amount of peptide adsorbed at monolayer coverage, is about 500 times lower than for the CH_3–SAM surface although the density of adsorption sites on this surface (i.e., the number of functional groups per unit area) is theoretically the same for both of these surfaces. As a result of this, for a given initial slope of the adsorption isotherm, which is equal to $QK/C°$ per eq 6, an artifactually low value of the *Q* parameter will result in an artifactually high value of *K*, with a corresponding overestimation of the strength of adsorption for the system per eq 17. The new method that we propose, however, keeps the *Q* and *K* parameters grouped together (as shown in eq 7) and uses them in a combined manner to estimate the initial slope of the adsorption isotherm where peptide–peptide interactions are minimized, thus avoiding their influence on the calculation of adsorption free energy.

The hydrophobic CH_3–SAM surface strongly adsorbed the TGTG-X-GTGT peptides with the trend in adsorption affinity being measured to be V > D > T. For a hydrophobic surface such as the CH_3–SAM, the driving force governing the adsorption behavior can be expected to depend most strongly on the overall hydrophobic characteristics of the peptide and the surface and the corresponding influence of this on the water structure at the interphase between the peptide and surface. Although still not fully understood, hydrophobic interactions are believed to originate from the perturbed structure of water molecules adjacent to nonpolar functional groups compared to the bulk solvent such that when two such functional groups are brought together part of this ordered hydration shell is released to the bulk solution with a corresponding increase in system entropy and subsequent decrease in free energy.[48] For our peptide model, the peptides differ only by the side-chain structure of the middle amino acid residue, and thus the characteristics of this residue can be expected to primarily dictate the differences in the observed adsorption behavior. The high affinity of the TGTG-V-GTGT peptide is consistent with expectations due to the nonpolar characteristic of valine (V) with its $\{–CH(CH_3)_2\}$ side group. The lower adsorption affinity of the peptide when aspartic acid (D) and theonine (T) amino acid residues were substituted for the middle residue can be explained by the relatively hydrophilic characteristics of these amino acid residues compared to those of valine, with D having a negatively charged side group and T having a polar side group. Both of these peptides, however, still exhibited fairly strong adsorption to the CH_3–SAM surface, which can be attributed to the presence of nonpolar functional groups (e.g., CH_2 and CH_3 groups) on each of the amino acids present in each of these peptides. On the basis of our previous molecular simulation studies[33] with similar peptide–SAM surface systems, we propose that the TGTG-D-GTGT and TGTG-T-GTGT peptides most likely adsorb to the CH_3–SAM surface with the hydrophilic components of the side groups of the D and T amino acid residues oriented away from the surface and facing out toward the aqueous solution, with the nonpolar components of the main-chain and the side-chain segments of the peptide adsorbed to the surface by hydrophobic interactions. We are currently conducting molecular dynamics simulation studies of these same peptide–SAM systems to provide further insights into the specific functional group interactions that may be occurring to elucidate the differences in the adsorption behavior of these peptides.

IV.c. Instrument Drift

The use of the raw SPR versus time plots shown in Figure 1 to generate the isotherm plots shown in Figure 2 requires that conditions of adsorption equilibrium are reached by the end of each sample injection period as evident by a plateau in the SPR versus time response curves. As shown in Figure 1, however, the SPR signal for each peptide continues to rise slightly after

the initial adsorption process occurs up until the time when pure buffer is injected to begin the desorption phase of the experiment. This continued rise in the SPR signal over time is believed to be due to instrument signal drift as opposed to being indicative of a failure to reach adsorption equilibrium.

To confirm that this rise was due to instrument drift, the rise in SPR signal versus time was calculated over the final 30 s of the peptide–sample injection period and compared with the rise in SPR signal versus time following the injection of a sample of pure buffer solution. The results from these pilot studies are presented in Table 5. As shown in this Table, the amount of instrument-signal drift for the peptide solutions is not significantly different from that of injections of pure buffer solution (p = 0.8214 and 0.5228 for the CH_3– and OH–SAMs, respectively), thus supporting the fact that this increase in the SPR signal over time following sample injection is indeed due to instrument drift and is not due to a failure of the adsorption processes to equilibrate during the adsorption experiments.

As shown in Table 5, the drift over the CH_3–SAM surface was found to be significantly higher than over the OH–SAM surface. Although we are uncertain about the exact cause of this phenomenon, we believe that it may result from differences in the structure of the solvent within these two very different interfacial environments. This can be expected to result in different values of the refractive index local to the surface and differences in the sensitivity of the refractive index to small changes in temperature, which could subsequently be reflected in differences in the SPR signal drift. Most importantly, for our concerns, this is a reproducible response that can be readily accounted for when using this instrument for peptide adsorption experiments.

IV.d. Reversible vs Irreversible Peptide and Protein Adsorption Behavior

As noted above, one of the essential conditions for the application of the proposed methods for the calculation of $\Delta G°_{ads}$ is that the adsorption process must be reversible, meaning that when the surface is exposed to the peptide-containing solution, the peptide molecules dynamically respond to the surface in a manner in which they are continually adsorbing to and releasing from the surface. Under these special conditions, the resulting shift in peptide concentration on the surface relative to the bulk solution can be related to the standard-state adsorption free energy for the system. Accordingly, if such a dynamic process is occurring and the surface is subsequently exposed to a peptide-free solution (i.e., pure bulk solvent), then the peptide must fully desorb from the surface because peptides are no longer present in solution to adsorb to the surface to replace the desorbing peptides. This is one of the primary telltale signs that can be used to indicate adsorption reversibility.

As clearly shown in many studies involving larger structured polypeptides (e.g., proteins), the adsorption process is generally found to be irreversible, especially on hydrophobic surfaces.[37,49] We believe that the difference between our model host–guest peptide and the general experience with protein adsorption is due to the relatively small size of the peptide, the resulting small number of functional group interactions involved, and the types of functional group interactions involved in the adsorption process. However, even for our relatively small, generally hydrophilic peptide, we have experienced guest residue types that result in irreversible adsorption. For example, when using alanine (A) as the guest residue over the CH_3–SAM surface, which has a single methylene side group, the adsorbed peptides did not desorb from the surface when the surface was flushed with bulk buffer solution within the time frame of our experiment (Figure 3). We therefore did not attempt to use this adsorption data to calculate the adsorption free energy for this system. These results suggest that, as a general rule, adsorption reversibility may be obtained for only fairly small peptides with few functional groups that strongly interact with the surface and that larger, structured polypeptides and

proteins with numerous functional group interactions should be expected to adsorb in an irreversible manner, especially on a hydrophobic surface.

IV.e. Relevance of Results to Protein Adsorption Behavior

The primary objective of this study was to develop an accurate experimental method that was sufficiently sensitive to be able to be used quantitatively to determine differences in adsorption behavior between different amino acid residues of a peptide and functional groups on a surface. Although these results cannot be directly used to predict the adsorption behavior of more complex structured proteins, which involve structural effects that are not represented in our model system, we do believe that the general trends in functional group interactions that are revealed from these studies should translate, at least qualitatively, to general trends that influence the adsorption behavior of proteins to surfaces. Furthermore, in addition to providing fundamental insights into these types of adsorption processes at the amino acid residue level, we are also very interested in using these data as a basis for the development of molecular simulation methods, which, once properly validated, should be able to be used to predict protein–surface interactions accurately.[33]

V. Conclusions

A new experimental method for the characterization of peptide adsorption has been developed using a peptide model in the form of TGTG-X-GTGT on functionalized SAM surfaces. This method was specifically designed for SPR spectroscopy to enable bulk-shift effects to be directly determined and to enable the standard-state adsorption free energy ($\Delta G°_{ads}$) to be calculated with minimal influence from peptide–peptide interactions at the adsorbent surface.

In this article, we present the first application of this method to characterize the adsorption behavior of a series of six different peptide–SAM systems (TGTG-X-GTGT with *X* = V, D, and T on CH_3– and OH–SAM surfaces). The results from these studies demonstrate that the developed method is sufficiently sensitive to determine significant differences for peptides adsorbed on different types of surfaces and between peptides on a given SAM surface with relatively minor differences in their amino acid sequence. This new method thus provides an excellent experimental platform to characterize the thermodynamics of adsorption for peptide–surface interactions. We are currently extending these methods to calculate $\Delta G°_{ads}$ for a broad range of additional peptide–SAM surface combinations.

In addition to providing insights into the fundamental adsorption behavior of peptides on functionalized surfaces, we will also be using the results of these studies as a benchmark data set for the evaluation, adjustment, and validation of force field parameters for the development of molecular simulation methods to enable protein–surface interactions to be accurately simulated and predicted. The ability to predict protein adsorption behavior accurately as a function of surface chemistry has applications to a broad range of problems in the fields of nanobiotechnology and biomedical engineering.

Acknowledgment

We gratefully acknowledge NIH for funding support for this research (NIBIB grant no. R01 EB006163). We also thank Dr. James E. Harriss of Clemson University for assistance with the various aspects of SPR biosensor chip fabrication for these studies and Ms. Megan Grobman, Dr. Lara Gamble, and Dr. David Castner of the University of Washington for assistance with surface characterization with XPS under the funding support of NIBIB (grant no. EB002027).

References

1. LatourRAWnekGBowlinGBiomaterials: Protein-Surface Interactions. The Encyclopedia of Biomaterials and BioengineeringTaylor & FrancisNew York Online update chapter for 2005 edition.
2. Kasemo B, Gold J. Adv. Dental Res 1999;13:8–20.
3. Puleo DA, Nanci A. Biomaterials 1999;20:2311–2321. [PubMed: 10614937]
4. Roach P, Farrar D, Perry CC. J. Am. Chem. Soc 2005;127:8168–8173. [PubMed: 15926845]
5. Agnihotri A, Siedlecki CA. Langmuir 2004;20:8846–8852. [PubMed: 15379516]
6. Vernekar VN, Latour RA. Mater. Res. Innovations 2005;9:337–353.
7. Sun Y, Dominy BN, Latour RA. J. Comput. Chem 2007;28:1883–1892. [PubMed: 17405115]
8. Latour RA, Christopher J, Rini J. J. Biomed. Mater. Res 2002;60:564–577. [PubMed: 11948515]
9. Norde W. Pure Appl. Chem 1994;66:491–496.
10. Sigal GB, Mrksich M, Whitesides GM. J. Am. Chem. Soc 1998;120:3464–3473.
11. Singh N, Husson SM. Langmuir 2006;22:8443–8451. [PubMed: 16981761]
12. Li X, Wei X, Husson SM. Biomacromolecules 2004;5:869–876. [PubMed: 15132675]
13. BIAtechnology Handbook. Biacore AB; Uppsala, Sweden: 1998. p. 4-1-4-4.
14. Jung LS, Campbell CT, Chinowsky TM, Mar MN, Yee SS. Langmuir 1998;14:5636–5648.
15. Charles, MR.; Abraham, ML. Quantitative Modeling of Protein Adsorption.. In: Malmsten, M., editor. Biopolymers at Interfaces. Vol. 2nd ed.. Marcel Dekker; New York: 2003. p. 71-94.
16. Hutchens TW, Yip TT, Porath J. Anal. Biochem 1988;170:168–182. [PubMed: 3389509]
17. Hutchens TW, Yip TT. Anal. Biochem 1990;191:160–168. [PubMed: 2077938]
18. Wirth HJ, Unger KK, Hearn MT. Anal. Biochem 1993;208:16–25. [PubMed: 8382018]
19. Bayramoglu G, Kaya B, Arica MY. Chem. Eng. Sci 2002;57:2323–2334.
20. Chern JM, Wu CY. Water Res 2001;35:4159–4165. [PubMed: 11791845]
21. Lan Q, Bassi AS, Zhu JX, Margaritis A. Chem. Eng. J 2001;81:179–186.
22. Sharma S, Argwal GP. Anal. Biochem 2001;288:126–140. [PubMed: 11152583]
23. Castellan, GW. Physical Chemistry. Vol. 3rd ed.. The Benjamin/Cummings Publ. Co.; Menlo Park, CA.: 1983. p. 347-351.Chapter 16
24. Adamson, AW. Physical Chemistry of Surfaces. Vol. 5th ed.. John Wiley & Sons, Inc.; New York: 1990. p. 421-423.
25. Mura-Galelli MJ, Voegel JC, Behr S, Bres EF, Schaaf P. Proc. Nat. Acad. Sci. U.S.A 1991;88:5557–5561.
26. Burns RA Jr. El-Sayed MY, Roberts MF. Proc. Nat. Acad. Sci. U.S.A 1982;79:4902–4906.
27. Morgan H, Taylor DM. Biosens Bioelectron 1992;7:405–410. [PubMed: 1515116]
28. Chase HA. J. Chromatogr 1984;297:179–202. [PubMed: 6436281]
29. Langmuir I. J. Am. Chem. Soc 1918;40:1361–1403.
30. Harpaz Y, Gerstein M, Chothia C. Structure 1994;2:641–649. [PubMed: 7922041]
31. Voet, D.; Voet, JG.; Pratt, CW. Fundamentals of Biochemistry. John Wiley & Sons; New York: 2002. p. 80-81.
32. Fournier, RL. Basic Transport Phenomena in Biomedical Engineering. Taylor & Francis; New York: 2007. p. 176
33. Raut VP, Agashe MA, Stuart SJ, Latour RA. Langmuir 2005;21:1629–1639. [PubMed: 15697318]
34. Anisimova MV, Shulga AA, Levichkin IV, Kirpichnikov MP, Polyakov KM, Skryabin KG, Vijayalakshmi MA, Varlamov VP. Russ. J. Bioorg. Chem 2001;27:23–46.
35. Gooding JJ, Mearns F, Yang W, Liu J. Electroanalysis 2003;15:81–96.
36. Bain C, Evall J, Whitesides GM. J. Am. Chem. Soc 1989;111:7155–7164.
37. NordeWHaynesCAHorbettTABrashJLProteins at Interfaces II: Fundamentals and Applications199560229American Chemical SocietyWashington, DC. ACS Symposium Series.
38. Tanahashi M, Matsuda T. J. Biomed. Mater. Res 1998;34:305–315. [PubMed: 9086400]
39. Pale-Grosdemange C, Simon ES, Prime KL, Whitesides GM. J. Am. Chem. Soc 1991;113:13–20.

40. Chang WS, Choi MJ, Kim JG, Cho SH, Whang KH. Int. J. Precision Eng. Manuf 2006;7:13–17.
41. Jenney CR, Anderson JM. J. Biomed. Mater. Res 1999;44:206–216. [PubMed: 10397922]
42. Sheller NB, Petrash S, Foster MD, Tsukruk VV. Langmuir 1998;14:4535–4544.
43. Cox JD, Curry MS, Skirboll SK, Gourley PL, Sasaki DY. Biomaterials 2002;23:929–935. [PubMed: 11771713]
44. Latour RA Jr. Hench LL. Biomaterials 2002;23:4633–4648. [PubMed: 12322985]
45. Latour RA Jr. Rini CJ. J. Biomed. Mater. Res 2002;60:564–577. [PubMed: 11948515]
46. Basalyga DM, Latour RA Jr. J. Biomed. Mater. Res. A 2003;64:120–130. [PubMed: 12483704]
47. Agashe M, Raut V, Stuart SJ, Latour RA. Langmuir 2005;21:1103–1117. [PubMed: 15667197]
48. KallayNColicMMillerJKallayNInterfacial Dynamics20003582Marcel DekkerNew YorkChapter 2 Surfactant Science Series
49. Koutsopoulos S, Patzsch K, Bosker WT, Norde W. Langmuir 2007;23:2000–2006. [PubMed: 17279687]

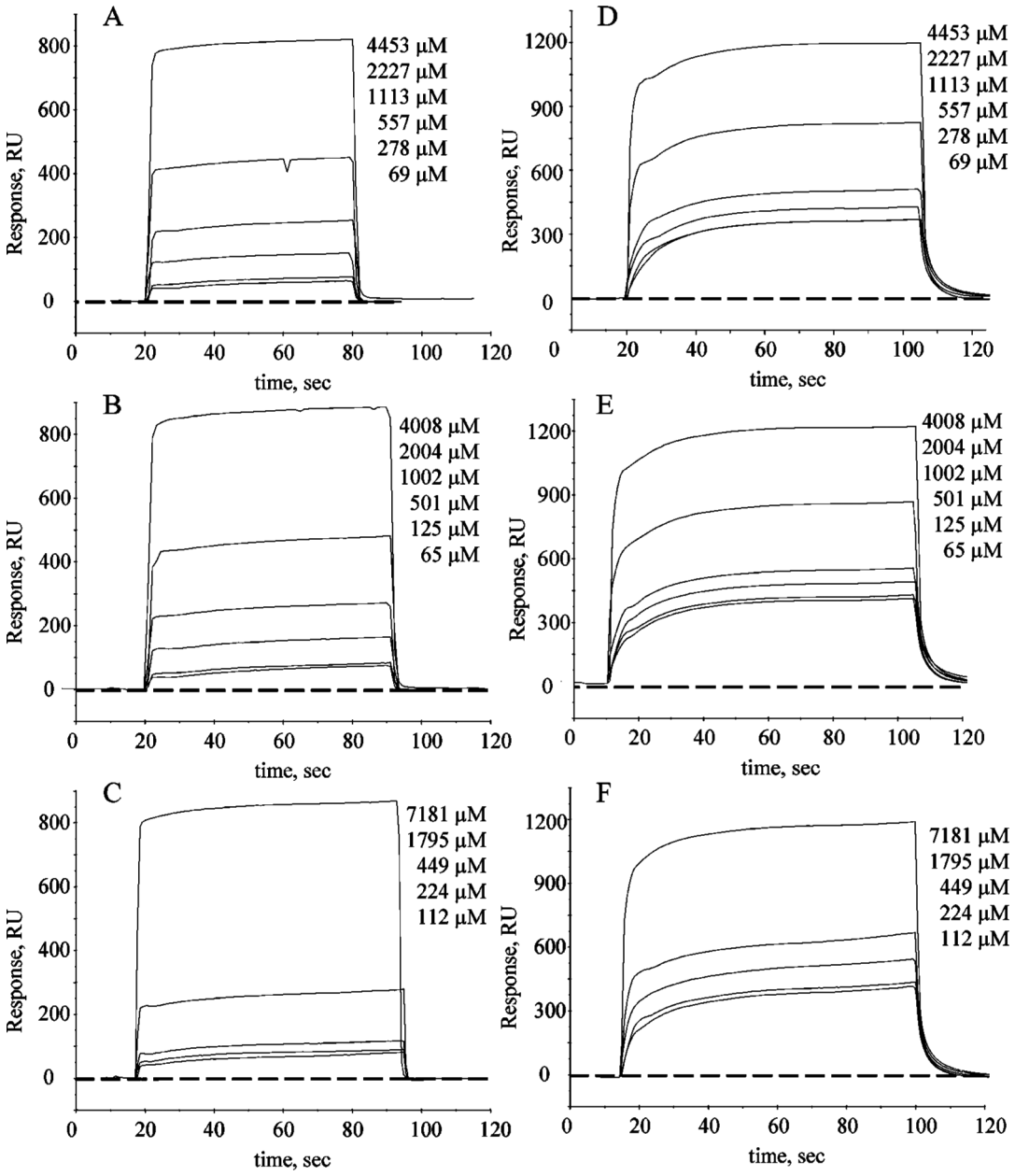

Figure 1.

Response curves (SPR signal (RU) vs time for TGTG-X-GTGT on OH– and CH_3–SAMs at 25 °C. (A) *X* = V, (B) *X* = D, and (C) *X* = T on the OH–SAM surface and (D) *X* = V, (E) *X* = D, and (F) *X* = T on the CH_3–SAM surface. (For clarity, not all of the concentration curves are listed for each peptide/surface pair because some of the low-concentration curves overlap one another and are thus not separately distinguishable).

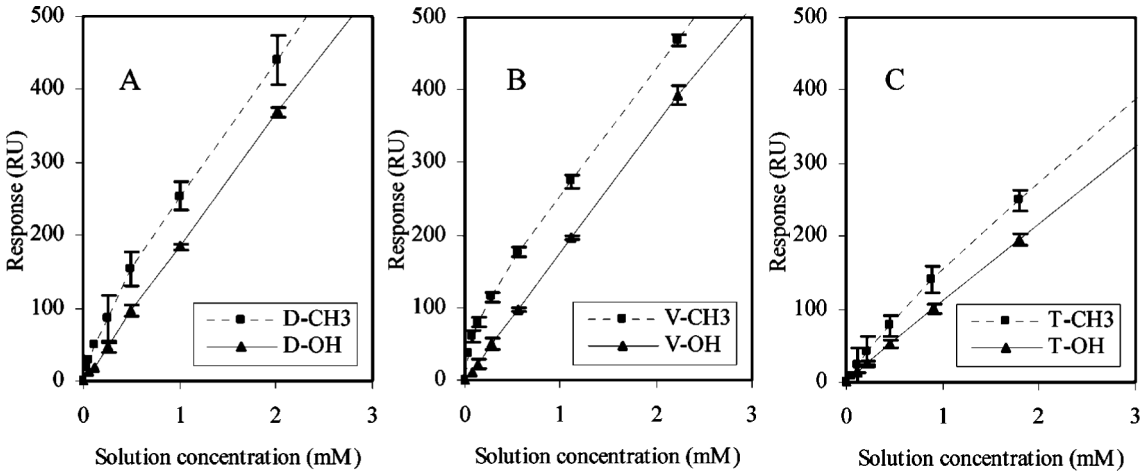

Figure 2.
Adsorption isotherms for TGTG-X-GTGT on the OH– and CH_3–SAM surfaces. (A) *X* = D, (B) *X* = V, and (C) *X* = T. The curves represent the best fit of eq 5 to the data points. Error bars represent 95% CI (*N* = 6).

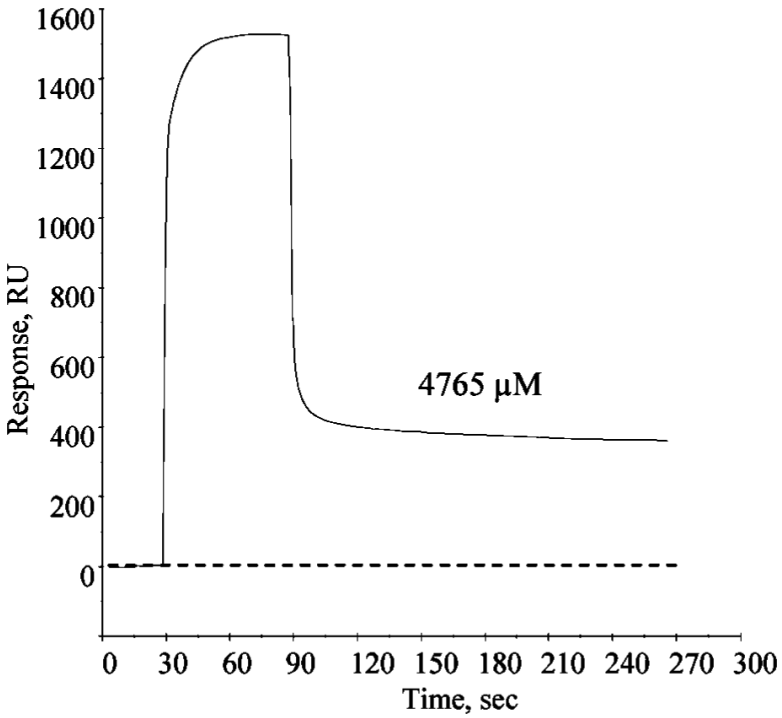

Figure 3.

Response curves (SPR signal (RU) vs time for TGTG-A-GTGT on CH_3–SAMs at 25° showing an irreversible adsorption process even for this small peptide. The large drop in the SPR response when pure buffer was introduced at 90 s is primarily due to the bulk-shift effect.

Table 1

Calculated Values of M_w and δ for Each Peptide

parameter	TGTG-D-GTGT	TGTG-T-GTGT	TGTG-V-GTGT
M_w (g/mol)	764.5	751.5	749.5
δ (Å)	12.1	12.0	12.0

Table 2

Contact Angle (DI Water in Air) and Ellipsometry Results (Layer Thickness) for the OH- and CH_3-Terminated Au—Alkanethiol SAM Surfaces (Mean ± 95% Confidence Interval (CI), $N = 3$)

SAM surface	contact angle (deg)	thickness (Å)
Au—$S(CH_2)_{11}$-OH	15.5 ± 2.1	13.0 ± 1.0
Au—$S(CH_2)_{11}$-CH_3	110.0 ± 3.0	11.0 ± 1.0

Table 3

Atomic Percentage (Composition) of OH- and CH_3-Terminated Au-Alkanethiol SAM Surfaces As Determined by XPS (Mean ± 95% CI, N = 3)

SAM surface	Au (%)	C (%)	S (%)	O (%)
Au—$S(CH_2)_{11}$-OH	33.1 ± 2.2	56.7 ± 3.0	2.8 ± 2.2	7.5 ± 0.9
Au—$S(CH_2)_{11}$-CH_3	32.3 ± 3.0	64.9 ± 2.6	2.8 ± 0.9	negligible

Table 4

Values of m, Q, K, ΔG^{o}_{ads}, and $\Delta G^{o}_{Langmuir}$ (Mean ± 95% CI) for Peptides on SAMs (N = 6)

	CH_3—SAM surface			OH—SAM surface		
	TGTGVGTGT	**TGTGDGTGT**	**TGTGTGTGT**	**TGTGVGTGT**	**TGTGDGTGT**	**TGTGTGTGT**
m (RU/M)	177 800 ± 3200	190 200 ± 7400	105 800 ± 2600	168 000 ± 17 000	171 900 ± 18 000	105 200 ± 10 400
Q (pg/mm^2)	79 ± 12	73 ± 20	94 ± 25	0.24 ± 0.11	0.15 ± 0.08	0.11 ± 0.06
K (unitless)	19 300 ± 9800	4940 ± 1980	1020 ± 470	14.4 ± 2.3	23.7 ± 7.8	19.0 ± 13.0
ΔG^{o}_{ads} (kcal/mol)	−4.40 ± 0.31	−3.54 ± 0.60	−2.76 ± 0.28	−0.002 ± 0.001	−0.003 ± 0.001	−0.001 ± 0.001
$\Delta G^{o}_{Langmuir}$(kcal/mol)	−5.85 ± 0.21	−5.04 ± 0.37	−4.10 ± 0.14	−1.58 ± 0.11	−1.88 ± 0.21	−1.75 ± 0.25

Table 5

Evaluation of Signal Drift (RU/s) for Each SAM Surface (Mean ± 95% CI; $N = 9$ for the Peptide Solutions, and $N = 3$ for the Pure Buffer Solutions)

signal drift (RU/s) on CH_3SAMs		signal drift (RU/s) on OH SAMs	
peptide solution	**buffer**	**peptide solution**	**buffer**
0.58 ± 0.08	0.60 ± 0.07	0.15 ± 0.03	0.14 ± 0.07